

EXPERIMENTAL EVALUATION OF DESIGN FEATURES OF A CRYOSTAT FOR AN IRON-LESS COSE SSC MAGNET

R. C. Wiemann, J. A. Carson, W. H. Engler, H. E. Fisk, J. D. Gonczy, R. H. Hanft, M. Kuchnir, P. M. Mantach, P. O. Mazur, A. D. McInturff, T. H. Nicol, J. Otavka, R. J. Powers, E. E. Schmidt, A. Szymulanski  
Fermilab National Accelerator Laboratory\*  
P. O. Box 500  
Batavia, Illinois 60510

A conceptual design for an iron-less cose SSC magnet cryostat has identified several areas for experimental study. Included are bowing of thermal radiation shields due to cooldown and warmup; thermal performance of the suspension systems; cryostat thermal performance; structural responses to decentering forces between the coil and the steel vacuum vessel; and response of thermal shields to forces due to quench induced eddy currents. Studies were carried out with 6m long thermal bowing and magnetic effects models, a suspension heat leak measurement dewar and a 12m long thermal model. The models incorporate important features of the conceptual cryostat design. The details of the test arrangements, procedures and results are presented.

Introduction

As a part of the Superconducting Super Collider (SSC) Reference Design<sup>1</sup> activity, Fermilab developed a design for an iron-less cose superconducting magnet system.<sup>2</sup>

The SSC is a 20 TeV on 20 TeV proton-proton collider having two adjacent 32 km diameter accelerator rings in a common tunnel. The rings are comprised of superconducting dipole, quadrupole and correction magnets.

The magnet system incorporates magnetically and cryogenically decoupled rings. The dipole magnets provide a 5T dipole field over a 5cm diameter, 12m long aperture. The magnet employs a Tevatron<sup>3</sup> style collared coil with warm iron at a large radius.

A conceptual cryostat design<sup>4,5</sup> was developed that allowed proper magnetic function, provided a low heat load to the refrigeration system, and was highly reliable at low cost. The cryostat section includes all required cryogenic lines and thus eliminates the need for external transfer lines. The lack of cold iron allows operational flexibility of the magnet system.

The design effort identified certain areas suitable for evaluation by experimental means. The results of the studies are, in general, applicable to other SSC cryostat designs. The significant elements of the experimental program are presented.

Thermal Bowing

The magnet cold mass and thermal radiation shields will be subjected to temperature gradients across their sections during the rapid cooldown and warmup cycles as required by the magnet system operational specifications. Such gradients result in bowing along the length of the magnet. The nature and magnitude of the bowing must be thoroughly understood for proper component design.

A program to study thermal bowing was developed and carried out. The objectives of the program were as follow:

- Verification of the dynamic behavior of a thermal shield during cooldown as predicted by a finite element model

\*Operated by Universities Research Association, Inc. under contract with the U. S. Department of Energy

- Development of a test facility for follow-on bowing and support response measurements

The cryostat's 10K thermal radiation shield was selected for study. The thermal and structural response of the shield, when subjected to an initial 100K temperature differential across the section, were modeled and predicted by finite element methods.

A test facility was developed to measure the thermal and structural response of the shield. The full size section, 6m long aluminum shield was instrumented for displacement and temperature measurement. Cooling was by means of a liquid nitrogen header on one side of the shield. The test was performed in air without a surrounding vacuum vessel. The test arrangement is shown in Figure 1.

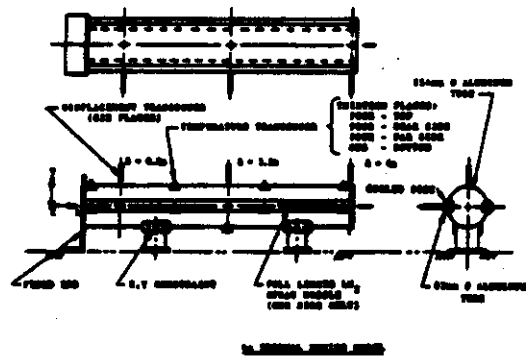


Figure 1

The displacement vs. time results are shown in Figure 2. Good agreement was achieved between the predicted and measured deflections. A -2.5cm maximum deflection was measured at the free end; i.e.,  $x = 6m$ , of the shield with the measured  $\Delta T$  across the shield being 120K.

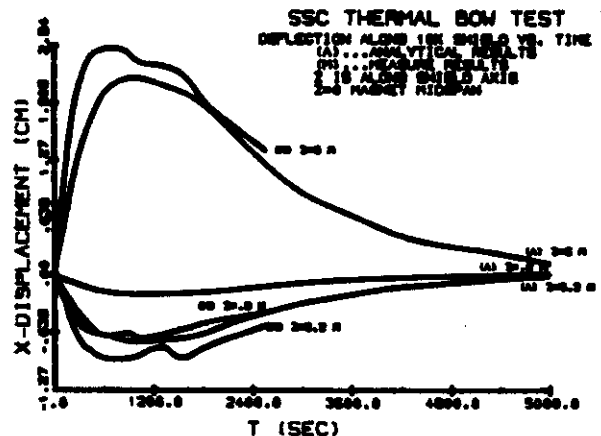


Figure 2

### Suspension Thermal Performance

The SSC refrigeration requirements are very stringent and result in low heat leak budgets. The heat leak contribution of the suspension system is significant and must be understood for cryostat design. Of particular importance is the ability to regularly achieve design performance levels.

A program to measure the heat leak of suspension systems was developed and carried out. The objectives of the program were as follows:

- . Develop a facility for the testing of cryostat component's: i.e., supports, insulation, valves, etc.
- . Measure the heat leak of cryostat components
- . Evaluate the effectiveness of thermal intercepts, connections, etc.

Critical to the measurement program is a liquid helium research dewar having a functionally adaptable test end that permits the evaluation of a wide variety of support geometries and sizes. The dewar provides for support member connections to the 4.5K end, to an intermediate temperature (10-40K) heat intercept, to an 80K heat intercept and to the 300K end. The dewar with a support member installed is shown in Figure 3.

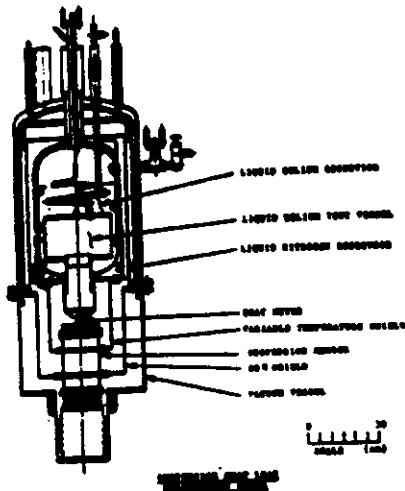


Figure 3

Measurement of a component's heat flow to its cold end is by means of a heat meter.<sup>6</sup> The heat meter employs a metallic reference section having a calibrated  $\Delta T$  across the section for heat flow as generated by a calibration heater at the warm end of the meter. The meter provides for accurate heat flow measurements with short time constants. The meter has been calibrated for both liquid helium and liquid nitrogen cold end temperatures with heat flows of 0-1 watt. Backup heat flow measurement is by conventional boil off methods.

A post type support member having construction details similar to those that could be applied to magnet suspensions was selected for evaluation. The post was designed to be compatible with the structural needs of the thermal and magnetic effects models. The post consisted of a single section FRP tube having shrink fit connections at the 4.5 and 300K ends and at the intermediate temperature and 80K heat intercepts. The post was instrumented to provide for temperature measurement at critical points along its length.

The heat leak and temperature distribution results are shown in Figure 4. The measured and predicted temperature profiles and heat leak to the cold end were in good agreement. The measured heat leak of 25mW to 4.5K demonstrates that small heat leaks to 4.5K can be achieved with conventional materials and methods.

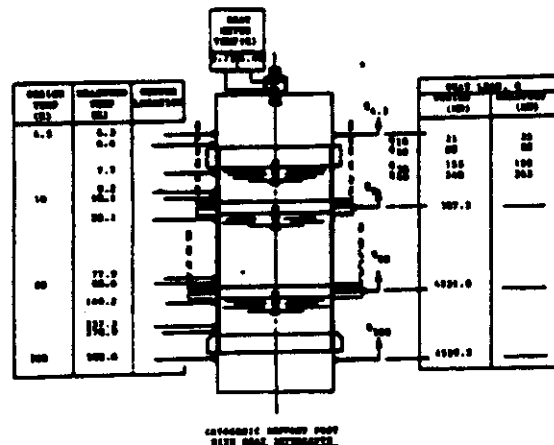


Figure 4

The thermal coupling as afforded by the shrink fit connections between the FRP tube and the metallic intercepts is very good as evidenced by the close correlation of the measured temperatures of the intercept and tube section above the intercept.

The facility will be used to evaluate other support members and is readily convertible for the measurement of the performance of multilayer insulation (MLI) systems.

### Cryostat Thermal Performance

The transition from a cryostat design to actual construction involves many details that have a significant effect on the thermal performance of the cryostat. Included are support fabrication and installation, heat intercept connections, MLI installation, vacuum pumpout, etc. The importance of understanding such details is amplified by the SSC requirements for a mass producible, low heat leak, low cost cryostat.

A program to design and construct a long dipole magnet type cryostat and to measure its thermal characteristics was developed and carried out. The objectives of the program were as follows:

- . Construct a 12m long cryostat
- . Understand cryostat fabrication tolerances
- . For a cryostat assembly; measure heat leaks to 4.5, 10 and 80K
- . Provide a test facility for follow-on heat leak measurements
- . Convertibility to an MTF compatible cryostat for magnetic testing of 12m coils

A 12m long thermal measurement model was designed and constructed. The center section of the model has a cold mass, aluminum 10K and 80K thermal shields and is contained in a vacuum vessel. The support members are the same as those evaluated by the suspension thermal performance measurements. The MLI consists of prefabricated blankets consisting of aluminized polyester film with fiberglass mat spacers.

Eleven layers of MLI are applied to the 10K surface and forty-four layers of MLI are applied to the 80K surface. The ends of the model are reservoirs that store the cryogens and provide the piping and instrumentation connections required for the thermal measurements. The model is shown in Figure 5.

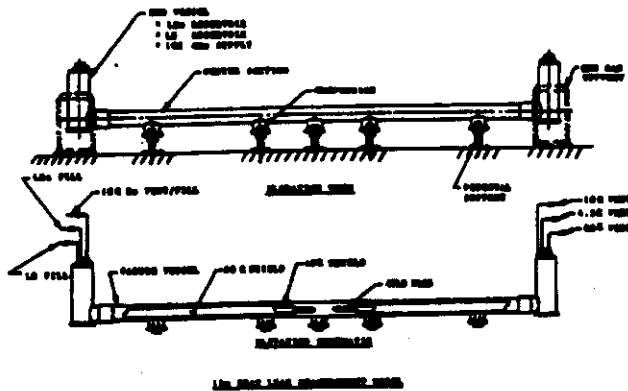


Figure 5

The heat leak measurements were made in an open cycle; i.e., no flow through the cold mass mode. The heat leak to 4.5K was determined by both measuring the liquid helium boiloff and measuring the temperature rate of rise of an aluminum thermal mass located within the cold mass shell. The rate of rise measurement was made with the 10K and 80K shields at temperature and after the helium had evaporated and the cold mass volume had been evacuated. The heat leak to 10K was determined by measuring the flow and temperature rise of the 10K shield gas stream. The heat leak to 80K was determined by measuring the liquid nitrogen boiloff. The 80K heat leak of the end vessels, which was measured previously, was subtracted to yield the net 80K heat leak to the center section.

Prior to the final assembly of the model, the end vessels were connected together in a closely coupled manner. The background heat gains of 22.0W to 80K and 450mW to 4.5K were determined by boiloff methods for this configuration.

The preliminary results of the thermal performance measurements are as given by Table 1.

PRELIMINARY THERMAL PERFORMANCE RESULTS

TABLE 1

| HEAT GAIN | ANALYTICAL PREDICTION           | MEASURED VALUE | MEASUREMENT METHOD          |        |
|-----------|---------------------------------|----------------|-----------------------------|--------|
| 80K       | End vessels (measured)          | 22.0W          | Boiloff                     |        |
|           | Thermal radiation (calculated)  | 8.3            |                             |        |
|           | Support conduction (calculated) | 21.2           |                             |        |
|           |                                 | 57.5W          | 95.5W                       |        |
| 10K       | Thermal radiation (calculated)  | 6.7W           | Gas stream temperature rise |        |
|           | Support conduction (calculated) | 1.52W          |                             |        |
|           |                                 | 2.28W          |                             | 2.28W  |
| 4.5K      | End vessels (measured)          | 450mW          | Boiloff                     |        |
|           | Thermal radiation (calculated)  | 2mW            |                             |        |
|           | Support conduction (calculated) | 1.75mW         |                             |        |
|           |                                 | 577mW          |                             | 1060mW |
|           |                                 | 577mW          |                             | 780mW  |

The measured steady state heat gain to the 80K shield was within 10% of the predicted value. This is reasonable agreement for this type of device. The steady state period was seven days.

The measured steady state heat gain to the 10K shield showed excellent agreement; i.e., to within -1% with the predicted value. The steady state period was two days. The heat gain to the 10K shield was also measured with the shield temperatures higher than 10K. Data at 15 and 28K show the anticipated reduction in heat leak to the shield.

The accurate measurement of the heat gain to the 4.5K liquid helium volume for such a large model is difficult. A very small heat gain for the center section of the model; i.e., ~127 mW, was predicted. This level can be easily dwarfed by the measured ~500 mW measurement background system. Two independent methods were employed to determine the heat gain to 4.5K. The helium boiloff method measured the overall boiloff the entire helium system; i.e., the center section, the end vessels, and connections. The preliminary results showed fair agreement between the measured (1060 mW) and predicted (577mW) steady state total heat gains. The steady state period was twelve hours. Further analysis will include corrections for shield operating temperatures, measured support heat gains and end effects. The rate of rise method measured the temperature rate of rise of the simulated coil; i.e., an aluminum plug, and the stainless steel cold mass containment vessel after the liquid helium was evaporated from the cold mass volume and the volume was evacuated with the 10K shield maintained at constant temperature. This method eliminates the measurement background contribution. The data is currently being analyzed.

The insulating vacuum during the measurement period was  $-1 \times 10^{-6}$  Torr.

Follow on measurements will include the effect of insulating vacuum on the performance of the MLI system between 300 and 80K.

### Magnetic Effects

The cryostat design identified several magnetic effects that result from the interaction of the magnet coil and cryostat components. Due to the long magnet length and the requirements of low cost and mass production, it was apparent the magnet coil would not be perfectly centered in the steel vacuum vessel that contains the fringe fields. The response of the suspension system and the deflection of the coil assembly due to the off-center forces needs to be understood. The relatively high conductivity aluminum thermal radiation shields will be affected by eddy current induced forces due to the quenching of the coil assembly. An understanding of deflections and corresponding stresses in the shields is important for proper design.

A program to design and construct and evaluate a magnetic effects model cryostat was developed and carried out. The objectives of the program were as follow:

- Construct an SSC style magnet
- Study fabrication techniques for coil and cryostat
- Understand cryostat component tolerances
- Measure mechanical and thermal response during cooldown
- Measure coil deflections due to off-center forces
- Measure eddy current induced motions during quench
- Map fringe fields

Eleven layers of MLI are applied to the 10K surface and forty-four layers of MLI are applied to the 80K surface. The ends of the model are reservoirs that store the cryogens and provide the piping and instrumentation connections required for the thermal measurements. The model is shown in Figure 5.

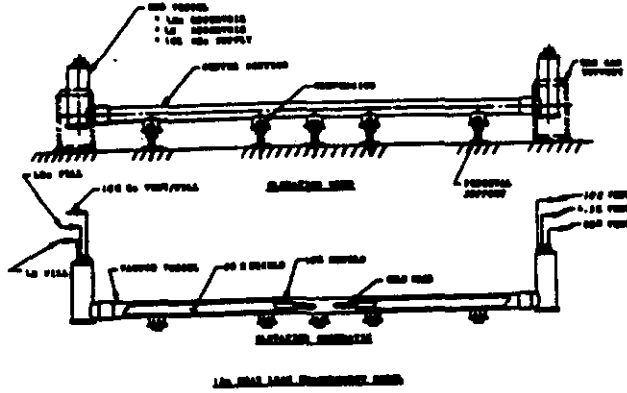


Figure 5

The heat leak measurements were made in an open cycle; i.e., no flow through the cold mass mode. The heat leak to 4.5K was determined by both measuring the liquid helium boiloff and measuring the temperature rate of rise of an aluminum thermal mass located within the cold mass shell. The rate of rise measurement was made with the 10K and 80K shields at temperature and after the helium had evaporated and the cold mass volume had been evacuated. The heat leak to 10K was determined by measuring the flow and temperature rise of the 10K shield gas stream. The heat leak to 80K was determined by measuring the liquid nitrogen boiloff. The 80K heat leak of the end vessels, which was measured previously, was subtracted to yield the net 80K heat leak to the center section.

Prior to the final assembly of the model, the end vessels were connected together in a closely coupled manner. The background heat gains of 22.0W to 80K and 450mW to 4.5K were determined by boiloff methods for this configuration.

The preliminary results of the thermal performance measurements are as given by Table 1.

PRELIMINARY THERMAL PERFORMANCE RESULTS

TABLE 1

| HEAT GAIN | ANALYTICAL PREDICTION             | MEASURED VALUE | MEASUREMENT METHOD                 |
|-----------|-----------------------------------|----------------|------------------------------------|
| 80K       | • End vessels (measured)          | 22.0W          | Boiloff                            |
|           | • Thermal radiation (calculated)  | 8.3            |                                    |
|           | • Support conduction (calculated) | 21.2           |                                    |
| 10K       | • Thermal radiation (calculated)  | 6.7W           | Gas stream temperature rise        |
|           | • Support conduction (calculated) | 1.5W           |                                    |
|           |                                   | 2.2W           |                                    |
| 4.5K      | • End vessels (measured)          | 450mW          | Boiloff                            |
|           | • Thermal radiation (calculated)  | 2mW            |                                    |
|           | • Support conduction (calculated) | 125mW          | Cold mass temperature rate of rise |
|           |                                   | 577mW          |                                    |
|           |                                   | 700mW          |                                    |

The measured steady state heat gain to the 80K shield was within 10% of the predicted value. This is reasonable agreement for this type of device. The steady state period was seven days.

The measured steady state heat gain to the 10K shield showed excellent agreement; i.e., to within -1% with the predicted value. The steady state period was two days. The heat gain to the 10K shield was also measured with the shield temperatures higher than 10K. Data at 15 and 28K show the anticipated reduction in heat leak to the shield.

The accurate measurement of the heat gain to the 4.5K liquid helium volume for such a large model is difficult. A very small heat gain for the center section of the model; i.e., ~127 mW, was predicted. This level can be easily dwarfed by the measured ~500 mW measurement background system. Two independent methods were employed to determine the heat gain to 4.5K. The helium boiloff method measured the overall boiloff the entire helium system; i.e., the center section, the end vessels, and connections. The preliminary results showed fair agreement between the measured (1060 mW) and predicted (577mW) steady state total heat gains. The steady state period was twelve hours. Further analysis will include corrections for shield operating temperatures, measured support heat gains and end effects. The rate of rise method measured the temperature rate of rise of the simulated coil; i.e., an aluminum plug, and the stainless steel cold mass containment vessel after the liquid helium was evaporated from the cold mass volume and the volume was evacuated with the 10K shield maintained at constant temperature. This method eliminates the measurement background contribution. The data is currently being analyzed.

The insulating vacuum during the measurement period was  $-1 \times 10^{-6}$  Torr.

Follow on measurements will include the effect of insulating vacuum on the performance of the MLI system between 300 and 80K.

Magnetic Effects

The cryostat design identified several magnetic effects that result from the interaction of the magnet coil and cryostat components. Due to the long magnet length and the requirements of low cost and mass production, it was apparent the magnet coil would not be perfectly centered in the steel vacuum vessel that contains the fringe fields. The response of the suspension system and the deflection of the coil assembly due to the off-center forces needs to be understood. The relatively high conductivity aluminum thermal radiation shields will be affected by eddy current induced forces due to the quenching of the coil assembly. An understanding of deflections and corresponding stresses in the shields is important for proper design.

A program to design and construct and evaluate a magnetic effects model cryostat was developed and carried out. The objectives of the program were as follow:

- Construct an SSC style magnet
- Study fabrication techniques for coil and cryostat
- Understand cryostat component tolerances
- Measure mechanical and thermal response during cooldown
- Measure coil deflections due to off-center forces
- Measure eddy current induced motions during quench
- Map fringe fields